Forest Chemicals Revew
www.forestchemicalsreview.com
ISSN: 1520-0191
July-August 2021 Page No. 958-973
Article History: Received: 12 May 2021 Revised: 25 June 2021 Accepted: 22 July 2021 Publication: 31 August 2021

Numerical Computation of Fractional PD Control System Based on the Shifted Fractional Legendre Functions

Yanjun Zhu, Cuirong Liu, Zhisheng Wu*, Ziting Hao
School of Electronic Information Engineering, Taiyuan University of Science and Technology, Taiyuan 030024, China
*Corresponding Author.

Abstract:

The numerical scheme of generalized fractional PD control system is established by using shift fractional Legendre function. The original differential equations model is transferred into a system of algebra equations by incorporating fractional differential operational matrices in the Caputo sense. Several test issues are presented to ensure that the proposed method is effective.

Keywords*: Fractional PD control system, Shifted fractional Legendre functions, Differential operational matrices, Numerical displacement solutions, Phase diagram.*

I. INTRODUCTION

Fractional calculus is frequently employed in mathematical modeling of physical responses, and its benefits have been demonstrated in a variety of scientific and engineering fields[1-8]. In the control process, the proportional-integral-derivative (PID) algorithms controller is the most preventive and simple closed-loop controller. To implement PID control, the deviation between the input and output values must be calculated, and the controlled device must be controlled using a linear combination of the deviation based on percentage, integral, and differential. The PID has three adjustable gains that need to be adjusted to achieve the desired response. In this paper, the general fractional PD control system is given as follows:

$$\lambda_n D^{p_n} X(t) + \lambda_{n-1} D^{p_{n-1}} X(t) + \ldots + \lambda_0 D^{p_0} X(t) = \gamma_m D^{q_m} Y(t) + \gamma_{m-1} D^{q_{m-1}} Y(t) + \ldots + \gamma_0 D^{q_0} Y(t) \qquad (1)$$

Where $D^{p} = {}_0^c D_t^{p}$, and $p_n > p_{n-1} > \cdots > p_0 \geq 0, q_m > q_{m-1} > \ldots > q_0 \geq 0$, p_k, γ_k are arbitrary numbers. The variable s is described by Laplace transform of Eq. (1) as

Forest Chemicals Revew
www.forestchemicalsreview.com
ISSN: 1520-0191
July-August 2021 Page No. 958-973
Article History: Received: 12 May 2021 Revised: 25 June 2021 Accepted: 22 July 2021 Publication: 31 August 2021

$$G(s)=\frac{\mathrm{X}(s)}{\mathrm{Y}(s)}=\frac{\gamma_m s^{q_m}+\gamma_{m-1}s^{q_{m-1}}+\cdots+\gamma_0 s^{q_0}}{\lambda_n s^{p_n}+\lambda_{n-1}s^{p_{n-1}}+\cdots+\lambda_0 s^{p_0}} \tag{2}$$

Initial conditions shall be met:

$$X(0)=X'(0)=\cdots=X^{(q-1)}(0)=0. \tag{3}$$

Several analytical and numerical methods for solving various fractional PID, PI or PD control systems are presented. Yumuk, et al. [9] utilize the Bode's ideal transfer function discuss the analytical design of fractional PID controller. Mandić, et al. [10] use the D-decomposition method obtain the dominant pole placement with fractional PID controller. Seyed, et al. [11] give the design of fractional PID controller for power system load frequency control (LFC) by using imperialist competition algorithm. Based on the above discussion, a numerical scheme is formulated to solve fractional-order PD control system using the shifted fractional Legendre functions.

The research paper is mainly composed of the following parts: Section 2 introduces basic definition of fractional calculus, and the shifted fractional Legendre function and its fractional differential operation matrix is given in Section 3. In Section 4, the solving process is established using the shifted fractional Legendre functions. Section 5 offers several numerical examples in order to demonstrate the effectiveness of method proposed. In Section 6, summarize the full text and draw a conclusion.

II. FRACTIONAL CALCULUS

In this part, the main points of fractional calculus theory will be introduced.

Definition 1. The definition of Riemann-Liouville formula of fractional differential operator is stated as

$$D_*^{\,p}X(s)=\begin{cases}\dfrac{1}{\Gamma(r-p)}\dfrac{d^r}{dt^r}\displaystyle\int_0^s\frac{X(s)}{(s-\varsigma)^{p-r+1}}d\varsigma & p>0,\ r-1\le p<r,\\ \dfrac{d^rX(s)}{ds} & p=r,s>0,\end{cases} \tag{4}$$

Definition 2. The Caputo formula of fractional differential operator is given by

Forest Chemicals Revew
www.forestchemicalsreview.com
ISSN: 1520-0191
July-August 2021 Page No. 958-973
Article History: Received: 12 May 2021 Revised: 25 June 2021 Accepted: 22 July 2021 Publication: 31 August 2021

$$ {}_{c}^{p}D\,X(s)=\begin{cases}\dfrac{1}{\Gamma(r-p)}\displaystyle\int_0^s\frac{X^{(r)}(s)}{(s-\varsigma)^{p-r+1}}d\varsigma, & r-1\le p<r;\\ \dfrac{d^rX(s)}{dt^r} & p=r,s>0;\end{cases} \tag{5} $$

For $p\ge 0,\sigma\ge -1$ and constant V, Caputo fractional derivative has the following basic properties:

(1) $D^{\,p}V=0;$

(2) $D^{\,p}s^{\sigma}=\begin{cases}0 & for\ \sigma\in N_0\ and\ \sigma<\lceil p\rceil;\\ \dfrac{\Gamma(\sigma+1)}{\Gamma(\sigma+1-p)}s^{\sigma-p}, & for\ \sigma\in N_0\ and\ \sigma\ge\lceil p\rceil\ or\ \sigma\notin N_0\ and\ \sigma>\lfloor p\rfloor;\end{cases}$

(3) $D^{\,p}\left(\sum_{i=0}^{r}\tilde{x}_iX_i(s)\right)=\sum_{i=0}^{r}\tilde{x}_iD^{\,p}X_i(s)$, where $\{\tilde{x}_i\}_{i=0}^{r}$ are constants.

Definition 3. (Generalized Taylor formula). Suppose that $D^{\,ip}X(s)\in[0,l]$ for $k=0,1,\ldots,r-1$, then

$$ X(s)=\sum_{k=0}^{r-1}\frac{s^{kp}}{\Gamma(kp+1)}D^{\,kp}X(0^{+})+\frac{s^{rp}}{\Gamma(rp+1)}D^{\,rp}X(\xi), \tag{6} $$

Where $0<\xi\le s,\forall s\in[0,l]$, also, one has

$$ \left|X(s)-\sum_{k=0}^{r-1}\frac{r^{kp}}{\Gamma(kp+1)}D^{\,kp}X(0^{+})\right|\le\Pi_r^p\frac{s^{rp}}{\Gamma(rp+1)}, \tag{7} $$

Where $\Pi_r^p\ge\left|D^{\,rp}X(\xi)\right|$.

When $p=1$, the generalized Taylor's formula is the best classical Taylor's formula.

III. SHIFTED FRACTIONAL LEGENDRE FUNCTIONS

Forest Chemicals Revew
www.forestchemicalsreview.com
ISSN: 1520-0191
July-August 2021 Page No. 958-973
Article History: Received: 12 May 2021 Revised: 25 June 2021 Accepted: 22 July 2021 Publication: 31 August 2021

In this part, the main points of shifted fractional Legendre functions will be introduced.

3.1 Generalized Fractional Legendre Functions

Fractional Legendre functions (FLFs) is defined by the transforming $t = v^p$ and $p > 0$ on shifted Legendre polynomials. The fractional Legendre functions are denoted by $FLF_k^p(v), k = 1, 2, \ldots$ They are the special solutions of the normalized eigenfunctions for the Liouville problem [12]

$$\left(\left(v - v^{1+p}\right) FLF_k^p(v)\right)' + p^2 k(k+1) v^{p-1} FLF_k(v) = 0, v \in [0,1]. \tag{8}$$

The function $FLF_k^p(v)$ is in a recursive form, as follows

$$FLF_{k+1}^p(v) = \frac{(2k+1)\left(2v^p - 1\right)}{k+1} FLF_k^p(v) - \frac{k}{k+k} FLF_{k-1}^p(v), k = 1, 2, \ldots \tag{9}$$

$$FLF_0^p(v) = 1, FLF_1^p(v) = 2v^p - 1. \tag{10}$$

Then the analytical form $FLF_k^p(v)$ of degree kv is derived as follows

$$FLF_k^p(v) = \sum_{s=0}^{k} \varpi_{s,k} v^{sp}, k = 0, 1, 2, \ldots, \tag{11}$$

Where $\varpi_{s,k} = \frac{(-1)^{k+s}(k+s)!}{(k-s)!(s!)^2}$ and $FLF_k^p(0) = (-1)^k, FLF_k^p(1) = 1.$

The FLFs are orthogonal to the weight function $w^p(v) = v^{p-1}$ on the interval $[0,1]$, then the orthogonal condition is

$$\int_0^1 FLF_n^p(v) FLF_m^p(v) w^p(v) dv = \frac{1}{(2n+1)p} \delta_{nm}, \tag{12}$$

Forest Chemicals Revew
www.forestchemicalsreview.com
ISSN: 1520-0191
July-August 2021 Page No. 958-973
Article History: Received: 12 May 2021 Revised: 25 June 2021 Accepted: 22 July 2021 Publication: 31 August 2021

Where δ_{nm} is the Kronecker function.

In order to use FLFs on the interval $[0,H]$, the generalized fractional Legendre functions (GFLFs), devoted by $FLF_k^{Hp}(t)$, is defined by introducing the change of variable $t=\nu H$. So the GFLFs have recurrence formula as follows

$$FLF_{k+1}^{Hp}(t)=\frac{(2k+1)\left(2(t/H)^p-1\right)}{k+1}FLF_k^{Hp}(t)-\frac{k}{k+1}FLF_{k-1}^{Hp}(t),\ k=1,2,\ldots, \tag{13}$$

Where $FLF_0^{Hp}(t)=1, FLF_1^{Hp}(t)=2(t/H)^p-1.$

The analytical form of the GFLFs $FLF_k^{Hp}(\nu)$ of degree kp is given by

$$FLF_k^{Hp}(t)=\sum_{s=0}^{k}\varpi_{s,k}\frac{t^{s\nu}}{H^{sp}},k=1,2,\ldots \tag{14}$$

Theorem 1. The GFLFs are orthogonal to the weight function $w^p(t)=t^{p-1}$ on the interval $[0,H]$, therefore the orthogonally condition is

$$\int_0^H FLF_n^{Hp}(t)FLF_m^{Hp}(t)w^p(t)dt=\frac{H^p}{(2n+1)p}\delta_{mn}. \tag{15}$$

Proof. With $\int_0^1 FLF_n^p(\nu)FLF_m^p(\nu)w^p(\nu)d\nu=\frac{1}{(2n+1)p}\delta_{nm}$, where δ_{nm} is the Kronecker function, let $\nu=\frac{t}{H}$, then

$$\begin{aligned}&\int_0^1 FLF_n^p(\nu)FLF_m^p(\nu)w^p(\nu)d\nu=\int_0^H FLF_n^p\left(\frac{t}{H}\right)FLF_m^p\left(\frac{t}{H}\right)w^p\left(\frac{t}{H}\right)\frac{1}{H}dt\\&=\int_0^H FLF_n^{Hp}(t)FLF_m^{Hp}(t)w^p(t)\frac{1}{H^p}dt=\frac{1}{(2n+1)p}\delta_{nm},\end{aligned} \tag{16}$$

Forest Chemicals Revew
www.forestchemicalsreview.com
ISSN: 1520-0191
July-August 2021 Page No. 958-973
Article History: Received: 12 May 2021 Revised: 25 June 2021 Accepted: 22 July 2021 Publication: 31 August 2021

$$\int_0^H FLF_n^{Hp}(t)\,FLF_m^{Hp}(t)\,w^p(t)\,dt=\frac{H^p}{(2n+1)\,p}\delta_{nm}. \tag{17}$$

The theorem is confirmed.

3.2 Function Approximation

Suppose $X(t)\in L^2[0,H]$, it can be extended by GFLF as follows:

$$X(t)=\sum_{k=0}^{\infty}\tilde{x}_i FLF_k^{hp}(t), \tag{18}$$

Where $\tilde{x}_k$ is obtained by

$$\tilde{x}_k=\frac{p(2k+1)}{H^p}\int_0^1 FLF_k^{Hp}(t)\,X(t)\,w^p(t)\,dt,\ k=0,1,2,\ldots \tag{19}$$

If truncated series are considered in Eq. (10), then

$$X(t)\approx X_r(t)=\sum_{k=0}^{r-1}\tilde{x}_k FLF_k^{hp}(t)=\mathbf{X}^T\mathbf{\Psi}(t), \tag{20}$$

Where

$$\mathbf{X}=[\tilde{x}_0,\tilde{x}_1,\ldots,\tilde{x}_{r-1}],\ \mathbf{\Psi}(t)=\left[FLF_0^{Hp}(t),FLF_1^{Hp}(t),\ldots,FLF_{r-1}^{Hp}(t)\right]. \tag{21}$$

Theorem 2. Suppose $D^{kp}X(t)\in C[0,H]$ *for* $k=0,1,2,\ldots,r-1(2r+1)\,p\geq 1$ and $\Theta_r^p=\text{span}\left\{FLF_0^{Hp}(t),FLF_1^{Hp}(t),\ldots,FLF_{r-1}^{Hp}(t)\right\}$. If $X_r(t)=\mathbf{X}^T\mathbf{\Psi}(t)$ is the best approximation to $X(t)$ from Θ_r^p, then the error bound is expressed as follows

$$\left\|X(t)-X_r(t)\right\|_w\leq\frac{\Pi_r^p}{\Gamma(rp+1)}\sqrt{\frac{H^p}{(2r+1)\,p}}, \tag{22}$$

Where $\Pi_r^p\geq\left|D^{rp}X(t)\right|, t\in[0,H]$.

Forest Chemicals Revew
www.forestchemicalsreview.com
ISSN: 1520-0191
July-August 2021 Page No. 958-973
Article History: Received: 12 May 2021 Revised: 25 June 2021 Accepted: 22 July 2021 Publication: 31 August 2021

Proof. Considering the generalized Taylor formula

$$X(t)=\sum_{k=0}^{r-1}\frac{t^{kp}}{\Gamma(kp+1)}D^{kp}X(0^{+})+\frac{t^{rp}}{\Gamma(rp+1)}D^{rp}X(\xi), \tag{23}$$

Where $0<\xi<t, t\in[0,H]$, with Definition 3

$$\left|X(t)-\sum_{k=0}^{r-1}\frac{t^{kp}}{\Gamma(kp+1)}D^{kp}X(0^{+})\right|\le\Pi_r^p\frac{t^{rp}}{\Gamma(rp+1)} \tag{24}$$

Since $X_r(t)=\mathbf{X}^T\boldsymbol{\Psi}(t)$ is the best approximation to $X(t)$ from Θ_r^p, and $\sum_{k=0}^{r-1}\frac{t^{kp}}{\Gamma(kp+1)}D^{kp}X(0^{+})\in\Pi_k^p$, hence

$$\begin{aligned}\left\|X(t)-X_r(t)\right\|_w^2&\le\left\|X(t)-\sum_{k=0}^{r-1}\frac{t^{kp}}{\Gamma(kp+1)}D^{kp}X(0^{+})\right\|\le\frac{\Pi_p^2}{\Gamma(rp+1)^2}\int_0^H t^{2rp}t^{p-1}dt\\&\le\frac{\Pi_p^2}{\Gamma(rp+1)^2}\int_0^H t^{(2r+1)p-1}dt=\frac{\Pi_p^2H^p}{\Gamma(rp+1)^2(2r+1)p}.\end{aligned} \tag{25}$$

Square roots prove the theorem. From the error bound, we can see the approximation convergence of GFLFs to the function $X(t)$.

3.3 GFLF operational matrix for derivatives

As the derivative of the function vector $\boldsymbol{\Psi}$ can be approximated

$$D^{p}\boldsymbol{\Psi}(t)\approx\mathbf{D}^{p}\boldsymbol{\Psi}(t), \tag{26}$$

$\mathbf{D}^p$ is defined as the GFLFs operational matrix of derivative.

Theorem 3. Supposingly, $\mathbf{D}^p$ is the $r\times r$ GFLFs operational matrix of Caputo fractional derivative of order $\gamma>0, p>\gamma/2, p\notin\square$, then the element of $\mathbf{D}^p$ are given as follows

Forest Chemicals Revew
www.forestchemicalsreview.com
ISSN: 1520-0191
July-August 2021 Page No. 958-973
Article History: Received: 12 May 2021 Revised: 25 June 2021 Accepted: 22 July 2021 Publication: 31 August 2021

$$\left\{d_{kj}\right\}_{k,j}^{r-1;r-1}=\left(2j+1\right)ph^{-\gamma}\sum_{s=0}^{k}\sum_{\upsilon=0}^{j}\varpi_{\upsilon,j}\varpi'_{s,k}\frac{\Gamma\left(sp+1\right)}{\Gamma\left(sp-\gamma+1\right)\left(s+p+1\right)p-\gamma},\tag{27}$$

Where

$$\varpi'_{s,k}=\begin{cases}0, & sp\in\square_0\ and\ sp<\gamma,\\ \varpi'_{s,k}=\varpi_{s,k}, & sp\notin\square_0\ and\ sp\geq\lfloor\gamma\rfloor\ or\ sp\in\square_0\ and\ sp\geq\gamma,\end{cases}\tag{28}$$

Proof. See [12].

IV. NUMERICAL SIMULATION

This section uses the fractional Legendre function of derivatives to convert the initial problem into a system of linear algebraic equations with initial conditions.

$$D^{p_n}X\left(t\right)\approx{}_0^cD_t^{p_n}\left(\mathbf{X}^T\mathbf{\Psi}\left(t\right)\right)\approx\mathbf{X}^T\mathbf{D}^{p_n}\mathbf{\Psi}\left(t\right),\tag{29}$$

$$D^{p_{n-1}}X\left(t\right)\approx{}_0^cD_t^{p_{n-1}}\left(\mathbf{X}^T\mathbf{\Psi}\left(t\right)\right)\approx\mathbf{X}^T\mathbf{D}^{p_{n-1}}\mathbf{\Psi}\left(t\right),\tag{30}$$

$$\vdots$$

$$D^{p_1}X\left(t\right)\approx{}_0^cD_t^{p_1}\left(\mathbf{X}^T\mathbf{\Psi}\left(t\right)\right)\approx\mathbf{X}^T\mathbf{D}^{p_1}\mathbf{\Psi}\left(t\right),\tag{31}$$

and

$$D^{q_n}Y\left(t\right)\approx{}_0^cD_t^{q_n}\left(\mathbf{Y}^T\mathbf{\Psi}\left(t\right)\right)\approx\mathbf{Y}^T\mathbf{D}^{q_n}\mathbf{\Psi}\left(t\right),\tag{32}$$

$$D^{q_{n-1}}Y\left(t\right)\approx{}_0^cD_t^{q_{n-1}}\left(\mathbf{Y}^T\mathbf{\Psi}\left(t\right)\right)\approx\mathbf{Y}^T\mathbf{D}^{q_{n-1}}\mathbf{\Psi}\left(t\right),\tag{33}$$

$$\vdots$$

$$D^{q_1}Y\left(t\right)\approx{}_0^cD_t^{q_1}\left(\mathbf{Y}^T\mathbf{\Psi}\left(t\right)\right)\approx\mathbf{Y}^T\mathbf{D}^{q_1}\mathbf{\Psi}\left(t\right),\tag{34}$$

Where Y can be obtained from Eq. (11). Substituting Eqs. (17)-(22) into Eq. (1), then

$$\begin{aligned}&\lambda_n\mathbf{X}^T\mathbf{D}^{p_n}\mathbf{\Psi}\left(t\right)+\lambda_{n-1}\mathbf{X}^T\mathbf{D}^{p_{n-1}}\mathbf{\Psi}\left(t\right)+\cdots+\lambda_0\mathbf{X}^T\mathbf{D}^{p_1}\mathbf{\Psi}\left(t\right)\\&=\gamma_m\mathbf{Y}^T\mathbf{D}^{q_n}\mathbf{\Psi}\left(t\right)+\gamma_{m-1}\mathbf{Y}^T\mathbf{D}^{q_{n-1}}\mathbf{\Psi}\left(t\right)+\cdots+\gamma_0\mathbf{Y}^T\mathbf{D}^{q_1}\mathbf{\Psi}\left(t\right)\end{aligned}\tag{35}$$

Forest Chemicals Revew
www.forestchemicalsreview.com
ISSN: 1520-0191
July-August 2021 Page No. 958-973
Article History: Received: 12 May 2021 Revised: 25 June 2021 Accepted: 22 July 2021 Publication: 31 August 2021

The flow chart of the provided algorithm is given in Fig. 1.

Forest Chemicals Revew
www.forestchemicalsreview.com
ISSN: 1520-0191
July-August 2021 Page No. 958-973
Article History: Received: 12 May 2021 Revised: 25 June 2021 Accepted: 22 July 2021 Publication: 31 August 2021

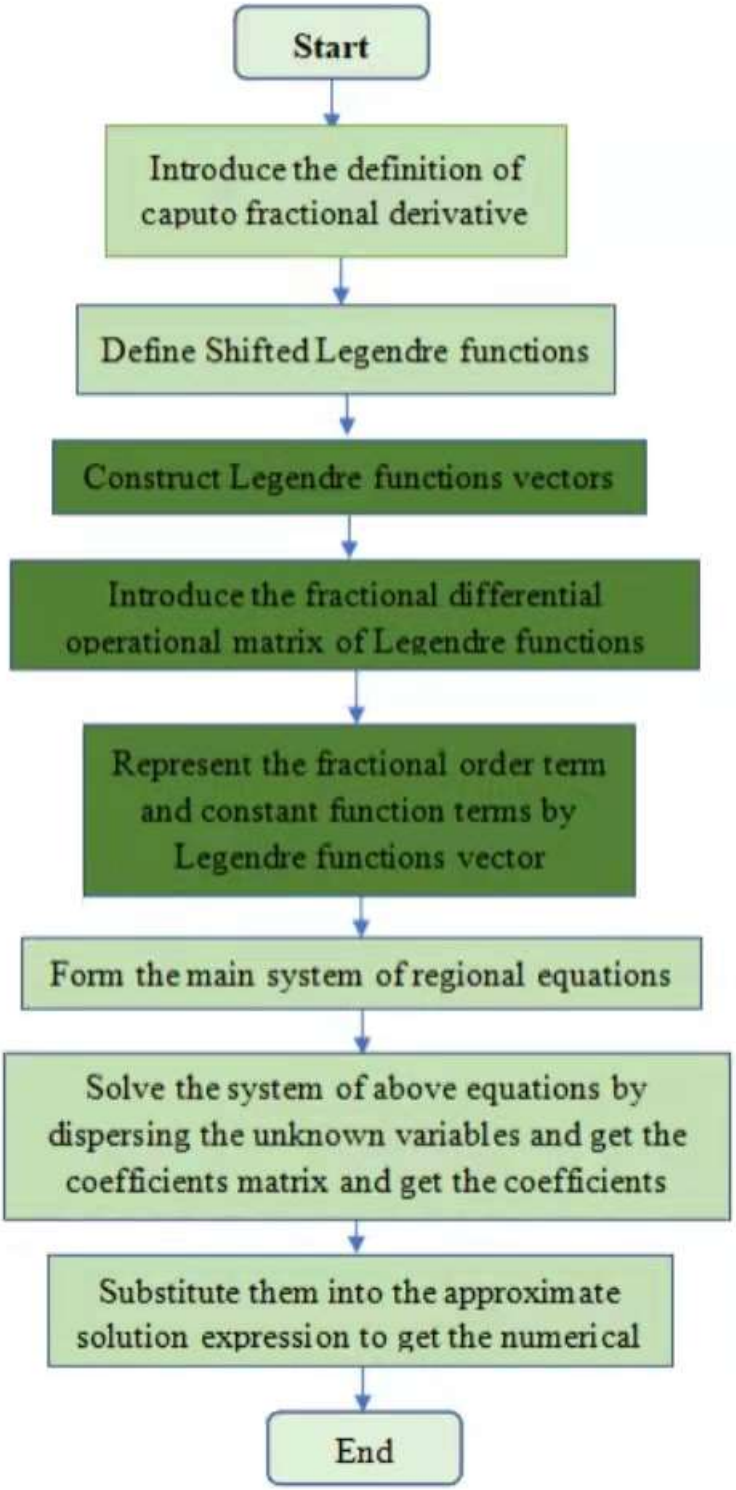

Forest Chemicals Revew
www.forestchemicalsreview.com
ISSN: 1520-0191
July-August 2021 Page No. 958-973
Article History: Received: 12 May 2021 Revised: 25 June 2021 Accepted: 22 July 2021 Publication: 31 August 2021

Fig.1: the flow chart of the algorithm

V. NUMERICAL EXAMPLES

Test problem 1. Considering the following fractional PD control system

$$2D^{3}X(t)+19D^{2.6}X(t)+35D^{1.4}X(t)+79D^{0.8}X(t)=58D^{2.3}Y(t)+90D^{1.2}Y(t)+117Y'(t) \quad (36)$$

Where the input signal is $Y(t)=\sin(t)$. When $m=4$ and 5, the displacement of the output signal and the phase position are illustrated in Fig.2 and Fig.3. From these two figures, it can be concluded that the numerical results are consistent when $m=4$ and 5, which shows that the proposed method is effective and accurate.

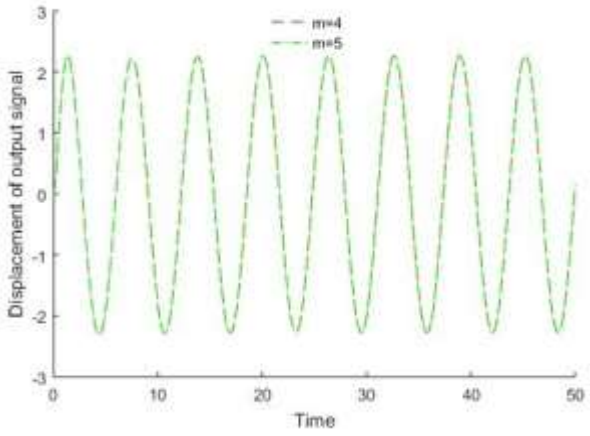

Fig.2: the displacement of output signal with $m=4$ and 5

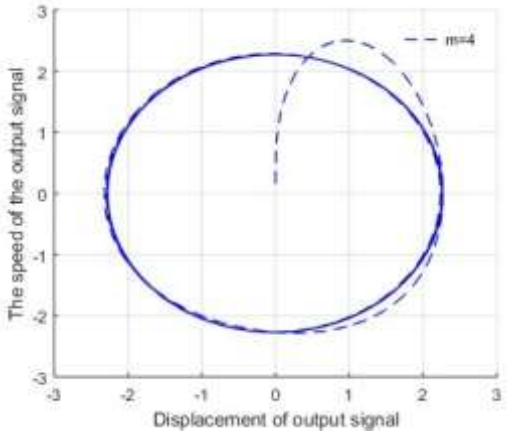

Forest Chemicals Revew
www.forestchemicalsreview.com
ISSN: 1520-0191
July-August 2021 Page No. 958-973
Article History: Received: 12 May 2021 Revised: 25 June 2021 Accepted: 22 July 2021 Publication: 31 August 2021

Fig.3: the phase position of output signal with $m=4$.

Test Problem 2. Considering the following fractional PD control system

$$D^{3.5}X(t)+8D^{3.1}X(t)+26D^{2.3}X(t)+73D^{1.2}X(t)+90D^{0.5}X(t)=30Y'(t)+90D^{0.3}Y(t), \quad (37)$$

where the input signal is $Y(t)=\sin(t^2)$, when $m=4$ and 5, the displacement of the output signal and the phase position are shown in Fig.4-Fig.5.

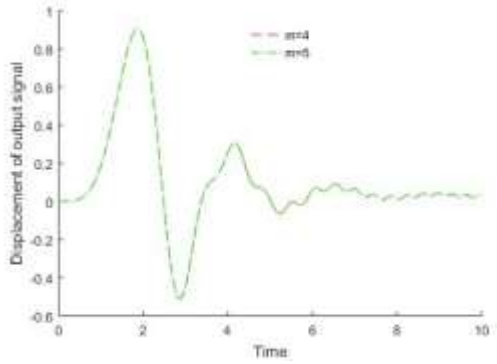

Fig.4: the displacement of output signal with $m=4$ and 5

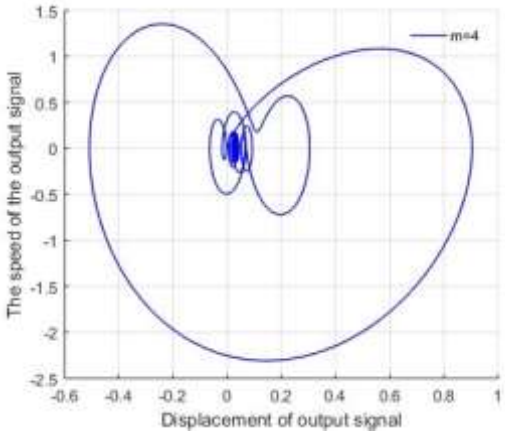

Fig.5: the phase position of output signal with $m=4$.

Test problem 3. Considering the following fractional PD control system

Forest Chemicals Revew
www.forestchemicalsreview.com
ISSN: 1520-0191
July-August 2021 Page No. 958-973
Article History: Received: 12 May 2021 Revised: 25 June 2021 Accepted: 22 July 2021 Publication: 31 August 2021

$$D^{1.2}X(t)+5D^{0.9}X(t)+9D^{0.6}X(t)+7D^{0.3}X(t)+2X(t)=Y(t) \tag{38}$$

Where the input signal is $Y(t)=\sin(\pi t)/(\pi t)$, $Y(t)=2e^{-1.5t}$ and $Y(t)=1, t>0; Y(t)=0, t<0$. When $m=4$, the displacement and phase position for three kinds of signals are shown in Fig.6-Fig.7.

Test problem4. Considering the following fractional PD control system

$$D^{2+p}X(t)+37D^{1+p}X(t)+79D^{p}X(t)+100X(t)=Y(t) \tag{39}$$

Where the input signal is $Y(t)=-\left[400\left(1-e^{-20t}\right)+100\sin(6\pi t)\right]$, When $m=4$, p=1, 0.8, 0.6, 0.4, the displacement of output signal is indicated in Fig.8 and the phase position is suggested in Fig.9.

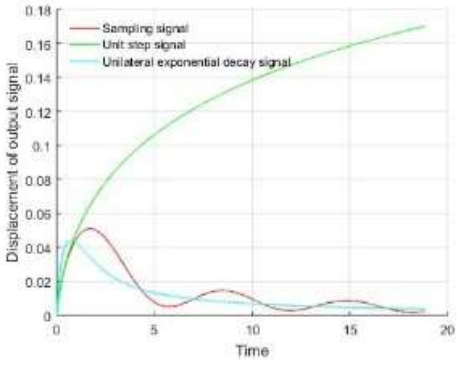

Fig.6: the displacement of three input signals with sampling signal, unit step signal and unilateral exponential decay signal when $m=4$

Forest Chemicals Revew
www.forestchemicalsreview.com
ISSN: 1520-0191
July-August 2021 Page No. 958-973
Article History: Received: 12 May 2021 Revised: 25 June 2021 Accepted: 22 July 2021 Publication: 31 August 2021

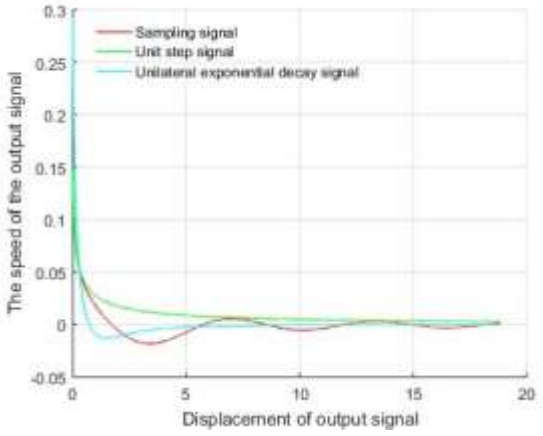

Fig.7: the phase position of three input signals with sampling signal, unit step signal and unilateral exponential decay signal when $m = 4$

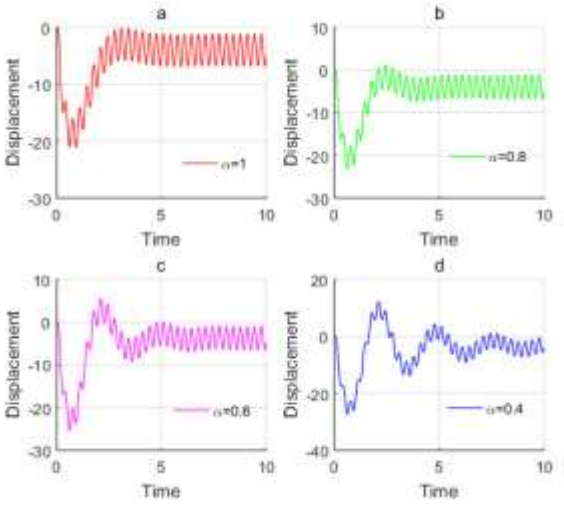

Fig.8: the displacement of output signals with p=1, 0.8, 0.6, 0.4

Forest Chemicals Revew
www.forestchemicalsreview.com
ISSN: 1520-0191
July-August 2021 Page No. 958-973
Article History: Received: 12 May 2021 Revised: 25 June 2021 Accepted: 22 July 2021 Publication: 31 August 2021

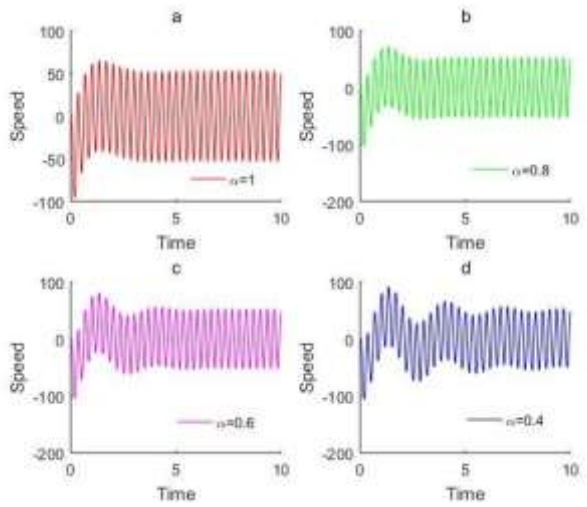

Fig.9: the phase position of output signal with p=1, 0.8, 0.6, 0.4

VI. CONCLUSION

In this paper, the researchers proposed a numerical scheme in an effort to solve the fractional PD control system by using the shift fractional Legendre function. The original system is converted into an array of linear algebraic equations by introducing the differential operation Matrix. Numerical examples show that the method is effective.

ACKNOWLEDGEMENT

The research work was funded by several projects, namely, the National Key Research and Development Project (No.2018YFA0707305), General program of National Natural Science Foundation of China (No.72071183), Key research and development projects in Shanxi Province (No.201903D321012), Shanxi equipment digitization and fault prediction Engineering Center Open project (ZBPHM-20201105).

REFERENCES

[1] Benkhettou N, Hassani S, Torres D (2016) A conformable fractional calculus on arbitrary time scales. Journal of King Saud University–Science

[2] Grzesikiewicz W, Wakulicz A, Zbiciak A (2013) Non-linear problems of fractional calculus in modeling of mechanical systems. International Journal of Mechanical Sciences 70: 90-98

Forest Chemicals Revew
www.forestchemicalsreview.com
ISSN: 1520-0191
July-August 2021 Page No. 958-973
Article History: Received: 12 May 2021 Revised: 25 June 2021 Accepted: 22 July 2021 Publication: 31 August 2021

[3] Mendes RV (2008) A fractional calculus interpretation of the fractional volatility model. Nonlinear Dynamics 55(4): 395-399

[4] Liang GS, Jing YM, Li ZE, et al. (2017) Modelling of frequency characteristics of the oil-paper compound insulation based on the fractional calculus. Iet Science Measurement & Technology 11(5): 646-654

[5] Carpinteri A, Cornetti P, Sapora A (2011) A fractional calculus approach to nonlocal elasticity. European Physical Journal Special Topics 193(1): 193-204

[6] Vázquez L (2005) A Fruitful Interplay: From Nonlocality to Fractional Calculus. Springer Netherlands

[7] Zhang L, Li J, Chen G (2005) Extension of Lyapunov second method by fractional calculus. Pure & Applied Mathematics, 21(3): 291-294

[8] Meilanov RP, Magomedov RA (2014) Thermodynamics in Fractional Calculus. Journal of Engineering Physics & Thermophysics 87(6): 1521-1531

[9] Yumuk E, Güzelkaya M, Eksin İ (2019) Analytical fractional PID controller design based on Bode's ideal transfer function plus time delay, ISA transactions

[10] Mandić PD, Šekara TB, Lazarević MP, et al. (2017) Dominant pole placement with fractional order PID controllers: D-decomposition approach, ISA transactions 67: 76-86

[11] Taher SA, Fini MH, Aliabadi SF (2014) Fractional order PID controller design for LFC in electric power systems using imperialist competitive algorithm. Ain Shams Engineering Journal 5(1): 121-135

[12] Klimek M, Agrawal OP (2013) Fractional Sturm-Liouville problem, Comput. Math. Appl. 66(5): 795-812.